

Stabilization of Copper(III) Ions with Deprotonated Hydroxyiminoamide Ligands: Syntheses, Structures, and Electronic Properties of Copper(II) and Copper(III) Complexes

Jan Hanss,^[a] Alexander Beckmann,^[a] and Hans-Jörg Krüger*^[a]

Keywords: Copper / Deprotonated amide ligands / Oxime ligands / Redox chemistry / High valent metal ions

Copper(II) and copper(III) complexes were prepared with two novel ligands, *N,N'*-bis(2-(1-hydroxyimino-2-methyl-1-phenyl)propyl)dimethylmalondiamide (*H₄mal55*) and *N,N'*-bis(2-(1-hydroxyiminoethyl)phenyl)dimethylmalondiamide (*H₄mal66*), both of which contain two amide and two oxime functionalities as potential ligand donor groups. The two copper(II) complexes (NEt₄)[Cu(*Hmal55*)] (**1**) and (NEt₄)[Cu(*Hmal66*)] (**2**) can be reversibly oxidized in acetonitrile at a redox potential of −0.120 and −0.075 V vs. the Fc/Fc⁺ redox couple, respectively. While the quantitative electrolysis of **1** results in the preparation of the oxidized complex [Cu(*Hmal55*)] (**3**), which is sufficiently stable to be isolated, isolation of the oxidation product of **2** was not attempted because of its long-term instability. The properties of the complexes were investigated by means of various spectroscopic methods (UV-vis, ESR, NMR, and IR

spectroscopy) and by X-ray structure analysis. The structure determinations and the spectroscopic investigations of the complexes reveal a square-planar CuN₄ coordination environment for each complex in the solid state and in acetonitrile solution. In both the oxidized and reduced oxidation states of the complexes, the coordinated ligands remain triply deprotonated with a hydrogen atom bridging both oxime oxygen atoms. The ligands can therefore be regarded as pseudo-macrocyclic. The characterization of the oxidation products clearly identifies the electron-transfer reaction as being metal-centered. For the first time, the structure of a copper(III) complex with a ligand containing oximes as donor groups was determined. The redox potentials of the copper complexes are compared to related Cu^{III}/Cu^{II} redox couples.

Introduction

The stability of highly oxidized metal ions in complexes is determined for the most part by the type of donor functions provided by the ligand. In general, anionic and highly polarizable donor groups are needed to achieve high oxidation states at the metal sites. For example, deprotonated amides as part of a multidentate ligand are well known to stabilize the trivalent oxidation state of the central ion in mononuclear copper and nickel complexes.^[1] Thus, copper(III) complexes have been synthesized and successfully isolated with ligands which contain carboxylate,^[2] amine,^[2] thiolate,^[3] alcoholate, and phenolate^[4] or further amide groups^[5] in addition to the deprotonated amide functions.

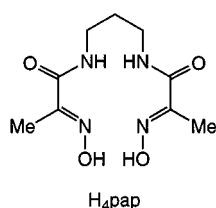
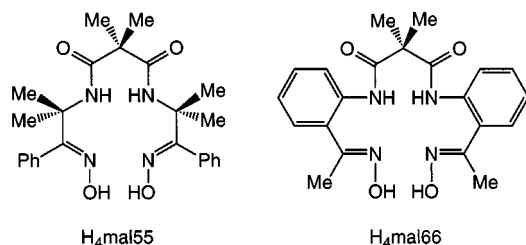
Another type of ligand donor function that has been demonstrated to generate high-valent metal ions is the deprotonated oxime group.^[6] While ligand systems with oximate groups produce stable nickel(III) and even nickel(IV) complexes,^[7] this ligand donor group seems to be considerably less well-established in the coordination chemistry of copper(III) ions. To our knowledge, the Cu^{III}/Cu^{II} redox chemistry has only been reported for two mononuclear copper complexes containing such ligand donor functions.^[8] In these complexes the metal ion is coordinated to two imine and two oxime nitrogen atoms in a square-planar geometry.

Further, since metal ions can be bound by the deprotonated oximate group via the nitrogen as well as via the oxygen atom, this type of ligand donor group has an advantage: multinuclear complexes which display interesting magnetic properties^[9] can be prepared and may, therefore, be potentially useful for the development of new materials in the field of molecular magnetism.^[10]

In light of the low Ni^{III}/Ni^{II} redox potentials obtained for nickel complexes with either amidate or oximate groups in the ligand environment,^[11] some years ago we initiated an investigation of the complexation properties of tetradentate ligands comprised of two deprotonated amide and two oxime groups. The ligands used in this study, *H₄mal55* and *H₄mal66*, are depicted below. They contain two amide and two oxime functions for the complexation of metal ions. Until recently^[12] complexes with such a combination of donor groups in a ligand were unknown. In a recent complexation study of copper(II) ions,^[12a] Kozłowski et al. employed the tetradentate amide-oxime ligand *H₄pap*, in which the oxime function is adjacent to the carboxylate portion of the amide group. In contrast, in both the acyclic amide-oxime ligands used in our investigation, the oximate groups lie on the side of the amine residues of the amide functions. In addition, the ligands *H₄mal55* and *H₄mal66* are designed to contain no hydrogen atom attached to a carbon atom in the α position to any donor atom; this feature has been shown to be very helpful in abolishing or at least in retarding possible decomposition reaction pathways of amidato complexes after the metal ion is oxidized.^{[2][13][14]} The two ligands *H₄mal55* and *H₄mal66* dis-

^[a] Institut für Anorganische und Angewandte Chemie der Universität Hamburg, Martin-Luther-King-Platz 6, D-20146 Hamburg, Germany
Fax: (internat.) +49(0)40/4123-2893
E-mail: krueger@xray.chemie.uni-hamburg.de

tinguish themselves by the different carbon chain lengths of the two hydroxyliminoamine components. Therefore, while ligand $H_4\text{mal55}$ is expected to form two five- and one six-membered chelate rings with the metal ion upon complexation, ligand $H_4\text{mal66}$ will render only six-membered chelate ring sizes.



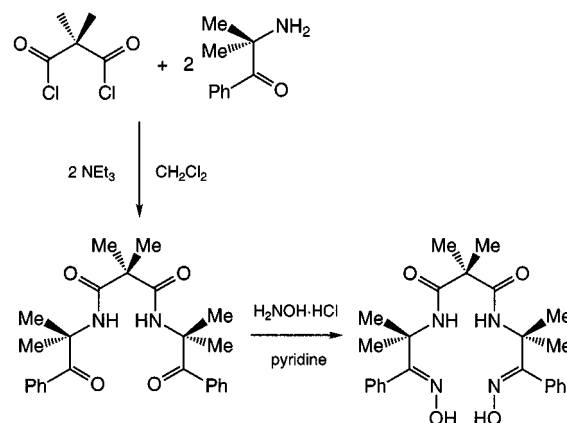
Here we introduce the results of the complexation reactions of the two novel amide-oxime ligands, $H_4\text{mal55}$ and $H_4\text{mal66}$, with copper ions, emphasizing the effects of the distinctive structural features of the ligands on the properties of the resulting complexes. The syntheses, as well as the structural and electronic properties of the copper(II) complexes, are described. The results of an electrochemical investigation, from which the isolation and first structural characterization of a copper(III) complex with oximate donor groups in the ligand environment ensued, are presented.

Results and Discussion

Preparation of the Ligands and the Copper(II) Complexes

Scheme 1 illustrates the synthesis of the ligand $H_4\text{mal55} \times 0.5 H_2O$, which was obtained from dimethylmalonyl dichloride and α -amino-isobutyrophenone in two reaction steps with an overall yield of 54%. Using a similar procedure, the ligand $H_4\text{mal66} \times H_2O$ was synthesized from dimethylmalonyl dichloride and 2-amino-acetophenone in a 62% overall yield.

The red copper(II) complexes $(Et_4N)[Cu(H\text{mal55})]$ (**1**) and $(Et_4N)[Cu(H\text{mal66})]$ (**2**) were prepared by refluxing the corresponding ligand with one equivalent of $Cu(OAc)_2 \times H_2O$ in the presence of two equivalents of $Et_4NOAc \times 4 H_2O$ in absolute ethanol. The elemental analyses of both compounds suggest that the coordinated ligand is triply deprotonated. The absence of N–H stretching vibrations between 3310 and 3370 cm^{-1} in the IR spectra of the complexes indicates that both amide nitrogen atoms are deprotonated upon complexation.



Scheme 1. Synthesis of the ligand $H_4\text{mal55}$

Structures of the Copper(II) Complexes

Perspective views of the copper(II) complex anions are displayed in Figures 1 and 2. A comparison of selected bond lengths and angles is listed in Table 1. In the crystal lattice of **1** $\cdot 0.5 Et_2O$, two crystallographically distinct, but otherwise chemically equivalent complexes are found. In both complexes **1** and **2**, the copper(II) ions are bound to two deprotonated amide and two oxime nitrogen atoms in essentially square-planar arrangements. The copper ions of the two symmetry-unrelated complex anions in the crystal lattice of **1** $\cdot 0.5 Et_2O$ deviate by 0.052 and 0.075 Å, respectively, from the calculated least-squares-plane of the four nitrogen donors. A similar deviation of the copper ion from the least-squares N_4 -plane (0.052 Å) is observed in **2**. In both complexes, the dihedral angle between opposing CuN_2 planes does not exceed 6.5°. The structure analysis of both copper(II) complexes provides further evidence that the two oximate oxygen atoms are bridged by a proton; this is in agreement with the previously mentioned elemental analyses and IR spectra. Similar to the crystal structure of the related complex anion $[Cu(H\text{pap})]^-$,^[12a] the hydrogen-bridging is found to be asymmetric. This feature of a hydrogen atom bridging both oximate oxygen atoms gives the ligands a pseudo-macrocyclic appearance with only six-membered chelate rings occurring in **2**, while in **1** the chelate ring sizes alternate between five and six. The interatomic O–O distance between the oxime oxygen atoms measures 2.427 ± 0.005 Å and 2.417 Å for **1** and **2**, respectively.

The different fused chelate-ring sizes have a profound effect on the degree of ruffling of the pseudo-macrocyclic ring as well as on the Cu–N bond lengths. Thus, while most of the atoms of the ligands backbone in **1** (except those of the methyl and the phenyl groups) lie approximately in the same plane as the CuN_4 unit, the ligand backbone in **2** exhibits a more saddle-like appearance in order to still be capable of accommodating the copper ion. The two phenylene rings in **2** are positioned under the CuN_4 plane, forming interplanar angles of 45.0–49.2° with the CuN_4 plane, while the two oxime oxygen atoms and the atoms of the malonyl bridge are located above the CuN_4 plane. Values of 36.5° and 31.7° are calculated for the interplanar angle

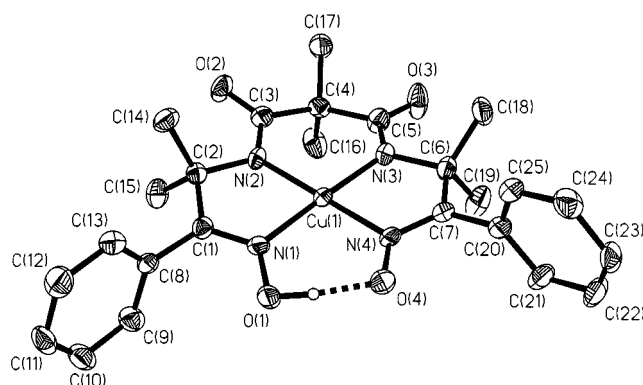


Figure 1. Perspective view of the structure of one of the two crystallographically independent $[\text{Cu}(\text{Hmal55})]^-$ anions in $\mathbf{1} \cdot 0.5 \text{ Et}_2\text{O}$ showing thermal ellipsoids at 50% probability and the atom-numbering scheme

enclosed by the CuN_4 -plane and the least-squares planes passing through the atoms N(2), C(9), C(11), and N(3) and through the atoms O(1), N(1), N(4), and O(4), respectively. In addition, the average $\text{Cu}-\text{N}_{\text{amide}}$ and $\text{Cu}-\text{N}_{\text{oxime}}$ distances in $\mathbf{1}$ of $1.906 \pm 0.005 \text{ \AA}$ and $1.950 \pm 0.011 \text{ \AA}$, respectively, increase to $1.946 \pm 0.006 \text{ \AA}$ and $2.000 \pm 0.011 \text{ \AA}$ in $\mathbf{2}$.

The $\text{Cu}-\text{N}_{\text{amide}}$ bond lengths compare well with those found in other square-planar amidato copper(II) complexes.^{[3][12a][15]} Reference values for $\text{Cu}-\text{N}_{\text{oxime}}$ distances in square-planar copper(II) complexes containing *vic* dioximate ligand donor groups are rare; the copper(II) ion is five-coordinate in most complexes with this type of donor function.^[16] The $\text{Cu}-\text{N}_{\text{oxime}}$ bond lengths (1.954 and 1.962 \AA) in the square-planar complex anion $[\text{Cu}(\text{Hpap})]^-$, which possesses the same sequence of fused chelate ring sizes as $\mathbf{1}$, resemble those observed in $\mathbf{1}$.^[12a]

Electronic Properties of the Copper(II) Complexes

The magnetic moments of $\mathbf{1}$ and $\mathbf{2}$ were determined to be 1.81 and $1.85 \mu_{\text{B}}$, respectively, which is consistent with the $S = 1/2$ state of the mononuclear copper(II) complexes. The ESR spectra of the complexes dissolved in an acetonitrile/toluene mixture ($v/v = 1:4$) and in pure ethanol were re-

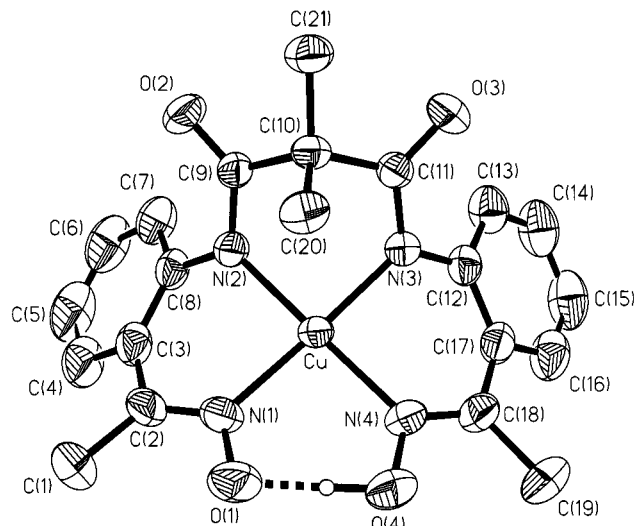


Figure 2. Perspective view of the structure of the $[\text{Cu}(\text{Hmal66})]^-$ anion in $\mathbf{2}$ showing thermal ellipsoids at 50% probability and the atom-numbering scheme. The location of the hydrogen atom which asymmetrically bridges both oxime oxygen atoms is disordered over two positions; the present view shows only one of these positions

corded at room temperature and at 100 K , respectively. The spectra are shown in Figure 3 and the ESR parameters obtained by simulation of the spectra are listed in Table 2. Thus, the solution of $\mathbf{1}$ at room temperature renders an isotropic ESR signal at $g_{\text{iso}} = 2.075$, which is split into four lines by the hyperfine coupling to the $I = 3/2$ spin of the copper nucleus. Further, superhyperfine splitting is observed due to the coupling to the nuclear spins $I = 1$ of the four nitrogen donor atoms of the ligand. The values for g_{iso} and $A^{\text{Cu}}_{\text{iso}} = 94.0 \cdot 10^{-4} \text{ cm}^{-1}$ are typical for square planar or for tetragonally elongated octahedral compounds of copper(II) ions with an equatorial N_4 -ligand donor environment. Through the interpretation of the powder spectrum of a frozen ethanolic solution of $\mathbf{1}$, one arrives at the same conclusion. Thus $g_z = 2.170$ and $A^{\text{Cu}}_z = 210 \cdot 10^{-4} \text{ cm}^{-1}$ have values that are predicted by a scatter plot of g_z vs. A^{Cu}_z for a monoanionic complex with a square planar or tetragonally distorted octahedral CuN_4 -coordination core.^[17] The g -values and the hyperfine coupling constants

Table 1. Selected bond lengths [\AA] and angles [deg] in $(\text{NEt}_4)[\text{Cu}(\text{Hmal55})]$ ($\mathbf{1}$), $(\text{NEt}_4)[\text{Cu}(\text{Hmal66})]$ ($\mathbf{2}$), and $[\text{Cu}(\text{Hmal55})]$ ($\mathbf{3}$)

	$(\text{NEt}_4)[\text{Cu}(\text{Hmal55})]^{[\text{a}]}$		$(\text{NEt}_4)[\text{Cu}(\text{Hmal66})]$	$[\text{Cu}(\text{Hmal55})]^{[\text{b}]}$
$\text{Cu}-\text{N}(1)$	1.940(4)	[1.951(4)]	2.010(2)	1.903(2)
$\text{Cu}-\text{N}(2)$	1.908(4)	[1.910(4)]	1.940(2)	1.860(2)
$\text{Cu}-\text{N}(3)$	1.901(4)	[1.906(4)]	1.951(2)	1.860(2) ^[\text{b}]
$\text{Cu}-\text{N}(4)$	1.961(4)	[1.949(4)]	1.989(2)	1.903(2) ^[\text{b}]
$\text{N}(1)-\text{Cu}-\text{N}(2)$	82.5(2)	[82.5(2)]	87.0(1)	83.1(1)
$\text{N}(1)-\text{Cu}-\text{N}(3)$	177.1(2)	[175.3(2)]	173.4(1)	175.4(1) ^[\text{b}]
$\text{N}(1)-\text{Cu}-\text{N}(4)$	93.9(2)	[94.5(2)]	94.1(1)	95.5(1) ^[\text{b}]
$\text{N}(2)-\text{Cu}-\text{N}(3)$	100.3(2)	[99.6(2)]	91.5(1)	98.0(1) ^[\text{b}]
$\text{N}(2)-\text{Cu}-\text{N}(4)$	173.3(2)	[174.4(2)]	178.8(1)	175.4(1) ^[\text{b}]
$\text{N}(3)-\text{Cu}-\text{N}(4)$	83.3(2)	[83.0(2)]	87.5(1)	83.1(1) ^[\text{b}]

^[\text{a}] The corresponding bond lengths and angles in the crystallographically distinct second complex anion in $\mathbf{1}$ are listed in square brackets. – ^[\text{b}] The atom numbering scheme of $[\text{Cu}(\text{Hmal55})]$ ($\mathbf{3}$) (cf. Figure 6) is adapted to that of $(\text{NEt}_4)[\text{Cu}(\text{Hmal55})]$ ($\mathbf{1}$). Thus, the atoms N(1') and N(2') in Figure 6 correspond to the atoms N(4) and N(3) in Table 1, respectively.

indicate further that the unpaired electron resides in the d_{xy} -orbital of the copper(II) ion if the coordinate system is arranged in such a way that the z axis lies perpendicular to the CuN_4 plane and the x axis bisects the $\text{N}_{\text{amide}}\text{--Cu--N}_{\text{amide}}$ angle. The ESR spectra of **2** have rather similar appearances except that the g_z value is slightly larger and the A^{Cu}_z value is smaller than that of **1**. A smaller g_z value and a larger A^{Cu}_z value is correlated to the greater ligand field strength that the ligand Hmal55^{3-} exerts on the copper ion. Thus, the ESR data confirm the presence of weaker Cu–N bonds in **2** as compared to those in **1**, a fact which has already been established by the structure determinations.

The electronic absorption spectra of the copper(II) complexes **1** and **2** are shown in Figure 4. The visible region of

the spectrum corresponding to **1** comprises two absorption bands at 405 and 509 nm. Based on their positions and intensities, the bands are attributed to d–d transitions. The energy range of the absorption bands indicates either that the coordination geometry observed in the solid state is preserved in solution or that any possible axial coordination by solvent molecules must be rather weak.^[18] Electrochemical evidence^[19] supports the notion that, in acetonitrile, solvent molecules are, if at all, extremely weakly coordinated to the axial coordination sites. Similar d–d transitions appear as shoulders with slightly higher intensities in the spectrum of **2**; the lower energies of the absorption bands agree with the previously stated proposition that a smaller ligand field strength is exerted by the ligand Hmal66^{3-} as compared to Hmal55^{3-} . The intense absorption around 280 nm is attributed to an amidato-to-copper(II) charge transfer transition.^[20]

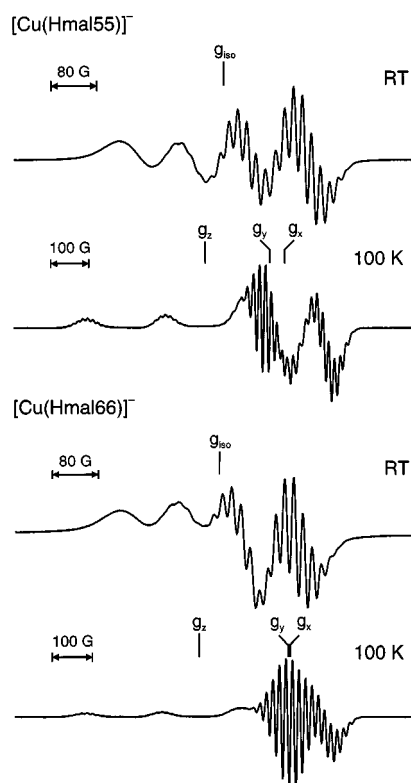


Figure 3. X-Band ESR spectra of $(\text{Et}_4\text{N})[\text{Cu}(\text{Hmal55})]$ (**1**) (top) and $(\text{Et}_4\text{N})[\text{Cu}(\text{Hmal66})]$ (**2**) (bottom) in acetonitrile/toluene ($\nu/\nu = 1:4$) at room temperature and as frozen glass in ethanol at 100 K (g -values are indicated)

Table 2. ESR properties of complexes **1** and **2** in acetonitrile/toluene mixture at room temperature and in frozen ethanol at 100 K

data	$(\text{NEt}_4)[\text{Cu}(\text{Hmal55})]$	$(\text{NEt}_4)[\text{Cu}(\text{Hmal66})]$
solution spectra at room temperature:		
g_{iso}	2.075	2.080
$A^{\text{Cu}}_{\text{iso}} (10^{-4} \text{ cm}^{-1})$	94.0	90.7
$A^{\text{N}}_{\text{iso}} (10^{-4} \text{ cm}^{-1})$	14.9	14.3
powder spectra at 100 K:		
g_x, g_y, g_z	2.037, 2.056, 2.170	2.046, 2.050, 2.200
$A^{\text{Cu}}_x, A^{\text{Cu}}_y, A^{\text{Cu}}_z (10^{-4} \text{ cm}^{-1})$	35.1, 33.9, 210	34.0, 28.9, 193
$A^{\text{N}}_x, A^{\text{N}}_y, A^{\text{N}}_z (10^{-4} \text{ cm}^{-1})$	16.1, 14.4, 13.6	15.9, 15.6, 14.0

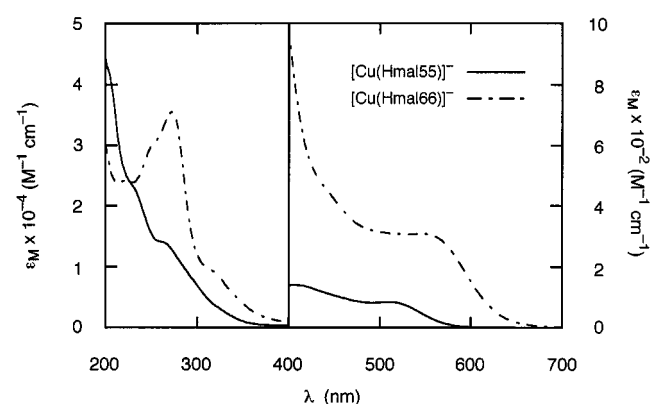


Figure 4. Electronic absorption spectra of the copper(II) complexes **1** and **2** in acetonitrile

Electrochemical Properties

The electrochemical properties of the copper(II) complexes were investigated by cyclic voltammetry and by coulometry in acetonitrile solution. The cyclic voltammograms of **1** and **2** are depicted in Figure 5. Both complexes reveal electrochemically reversible oxidation reactions (the current ratio $|i_{\text{p,a}}/i_{\text{p,c}}| \approx 1$; $i_{\text{p}}/\nu^{1/2}$ and the separation of the peak-potentials ΔE_{p} are independent of the scan rate ν) at -120 and -75 mV vs. the ferrocene/ferrocenium (Fc/Fc^+) redox couple in acetonitrile, respectively. No reversible reductions are observed. Coulometric oxidations of the complexes at an applied potential of 80 mV for **1** and 125 mV for **2** produce dark brown-red solutions. Quantitative electrolysis demonstrates that the complexes are oxidized by one electron; immediate re-reduction results in the recovery of 98 and 95% of the reduced complexes **1** and **2**. The long-term stability of the oxidized species was examined spectrophotometrically. Thus, 95% of the oxidation product of **1** are still present after 3 d and 91% after six days, indicating that isolation of the oxidized compound should be feasible. In contrast, only 67% and 51% of the oxidized species of **2** can be detected after 3 and 6 d, respectively.^[21] Due to this

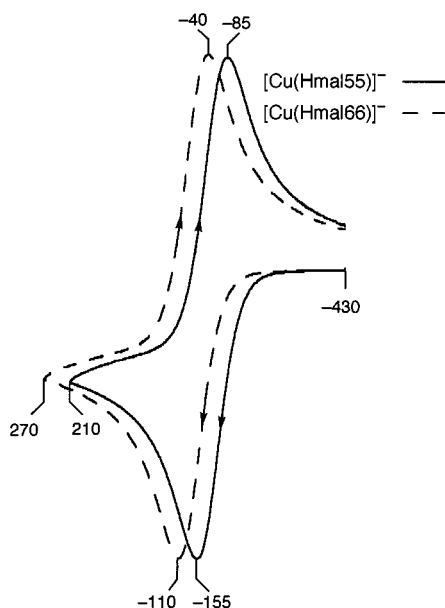


Figure 5. Cyclic voltammograms (50 mV/s) of **1** (solid line) and **2** (dashed line) at a Pt-foil electrode in acetonitrile at room temperature; peak potentials in mV vs. Fc/Fc^+ redox couple are indicated

apparent instability, no isolation of the oxidation product of **2** was attempted.

In water containing 0.05 M $\text{NEt}_4(\text{ClO}_4)$ as supporting electrolyte, the oxidation potentials for **1** and **2** were determined to be 750 and 770 mV vs. NHE, respectively. The electrochemical behavior of the complexes in water is, however, less ideal than that in acetonitrile, as demonstrated by the peak current ratio and by the incipient appearance of adsorption phenomena for the oxidation product of **1**. Addition of NEt_4OH effectuates a shift of the potential of **2** by 60 mV to a more negative value, indicating that the coordinated ligand loses its bridging proton in a more basic medium. However, the shape of the electrochemical response demonstrates decomposition of the oxidized species; for **1** oxidation was no longer observed upon addition of base; this means that the stability of the fully deprotonated copper(II) complex $[\text{Cu}(\text{mal55})]^{2-}$ is very limited in water.

Preparation of Copper(III) Complexes

Indeed, consecutive coulometric oxidation of complex **1** in acetonitrile, evaporation of the acetonitrile, and recrystallization of the obtained residue from toluene/hexane affords analytically pure product. The elemental analysis of the compound is consistent with its formulation as $[\text{Cu}(\text{Hmal55})]$ (**3**). The IR spectrum of **3** is very similar to that of **1** except that the features corresponding to the counter cation NEt_4^+ are now absent. For the purpose of comparing spectroscopic data, solutions of the oxidation product of **2** were electrochemically generated in situ and, in light of the apparent instability of the oxidized species, immediately used for the respective measurements.

Structure of the Copper(III) Complex $[\text{Cu}(\text{Hmal55})]$

A crystal structure determination was carried out on a single crystal of **3**. A perspective view of the complex is presented in Figure 6. In Table 1 some selected bond lengths and angles of compound **3** are compared to those of the reduced complex. Overall, the ligand environment, as well as the coordination geometry at the center ion, is preserved upon oxidation of **1**. The copper ion in **3** deviates by approximately the same amount (0.073 Å) from the least-squares N_4 -plane as in **1** and also the dihedral angles between opposing CuN_2 -planes are still under 6.5° . The structure analysis provides evidence that the H-bridging between the oxime oxygen atoms still persists in complex **3**. Compared to complex **1**, the Cu–N distances are reduced by 0.05 Å, indicating metal-centered oxidation. The decrease of the copper-donor atom bond lengths upon oxidation of the metal ion is, however, considerably smaller than that observed in other square-planar copper(II)/copper(III) couples with acyclic ligands.^[2,3,5] In our opinion, the modest reduction of Cu–N bond lengths, despite the loss of a strongly σ -antibonding electron, can be attributed to the pseudo-macrocyclic nature of the coordinated ligand, which does not allow a tighter enclosure of the metal ion by the ligand without introduction of steric strain on the ligand backbone. A closer inspection of the structural parameters of the ligand reveals no major differences between complex **1** and **3** except that the ruffling of macrocyclic ring seems to be a little bit more pronounced in the oxidized complex. This observation is also manifested by the rather small decrease of the interatomic O–O distance between the oxime oxygen atoms from 2.427 ± 0.005 Å in **1** to 2.400 Å in **3**. The $\text{Cu}^{\text{III}}\text{--N}_{\text{amide}}$ bond length of 1.860 Å is at the high end of the range of values observed for a bond length between a copper(III) ion and a deprotonated amide nitrogen donor atom.^[2–5]

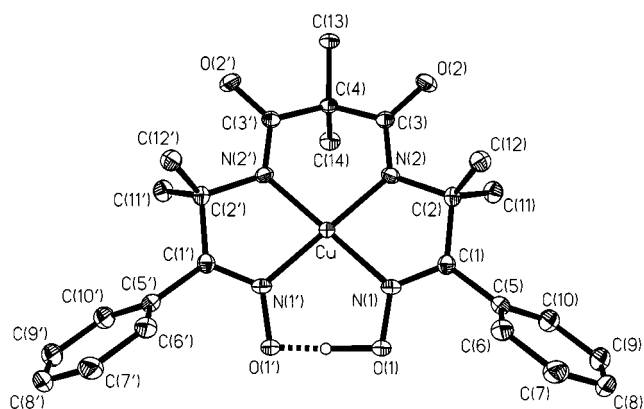


Figure 6. Perspective view of the structure of $[\text{Cu}(\text{Hmal55})]$ (**3**) showing thermal ellipsoids at 50% probability and the atom-numbering scheme. The location of the hydrogen atom which asymmetrically bridges both oxime oxygen atoms is disordered over two positions; the present view shows only one of these positions

As previously noticed for other amidato copper(III) complexes,^[2–5] in response to the higher positive charge on the copper ion upon oxidation, the partial double bond charac-

ter of the C–N bond in the deprotonated amide function is reduced in order to provide the amide nitrogen atom with a higher negative charge. Thus, the average C–N and C–O bond lengths change from 1.325 and 1.240 Å in **1** to 1.358 and 1.233 Å in **3**, respectively. The strengthening of the C–O bond upon oxidation of the metal ion is accompanied by an increase of the C=O stretching frequency by 28 cm⁻¹ in the IR spectra.

Spectroscopic Properties of the Copper(III) Complex

The diamagnetism of complex **3** which would be expected for a complex with a copper(III) ion is confirmed by NMR spectroscopy. The NMR spectrum of **3** in CD₂Cl₂ clearly establishes that the ligand is still bound to the metal ion in its triply deprotonated form, i.e. the oxime oxygen atoms are still bridged by a proton. A similar result is obtained when the oxidation product of **2** is examined by NMR spectroscopy immediately after its electrochemical generation.

Addition of a base like triethylamine to a solution of complex **3** in deuterated acetonitrile or dichloromethane seems to cause deprotonation of the oxime group, which is, however, accompanied by decomposition reaction(s) of the complex.

Intense absorption bands with extinction coefficients between 1000 and 8000 M⁻¹ cm⁻¹ are present in the visible regions of the electronic absorption spectra of both oxidized complexes (Figure 7). These bands are tentatively attributed to LMCT transitions. In general, two strong absorption bands are observed in the spectra of copper(III) peptide complexes at 260–280 nm and at 380–400 nm attributed to the σ and π N(peptide)-to-copper(III) charge transfer transitions, respectively.^[1,22] Copper(III) imine-oximate complexes yield a LMCT band between 515 and 581 nm. The absorption bands in the electronic absorption spectra of the complexes [Cu(Hmal55)] and [Cu(Hmal66)] occur at rather similar energies. Except for the intense band around 773 nm for [Cu(Hmal66)], the visible regions in the spectra of both oxidized complexes resemble each other. The reason for the additional appearance of an intense band around 773 nm for [Cu(Hmal66)] is attributed to a LMCT transition involving the phenylene moieties of the ligand. Such LMCT transition are likely to occur with the oxidized copper ion in [Cu(Hmal66)], since here the sp²-hybridized donor atoms are part of π -molecular orbital systems extending over the phenylene units.

Comparison of Redox Potentials

In Figure 8a, the redox potentials of compounds **1** and **2** are compared with those of some selected copper complexes in aqueous solutions. With the exception of complex **12**,^[8a] all complexes contain at least two deprotonated amide functions as ligand donor groups, while complexes **1**, **2**, and **12** possess two vicinal dioximate ligand donor groups as a common feature.

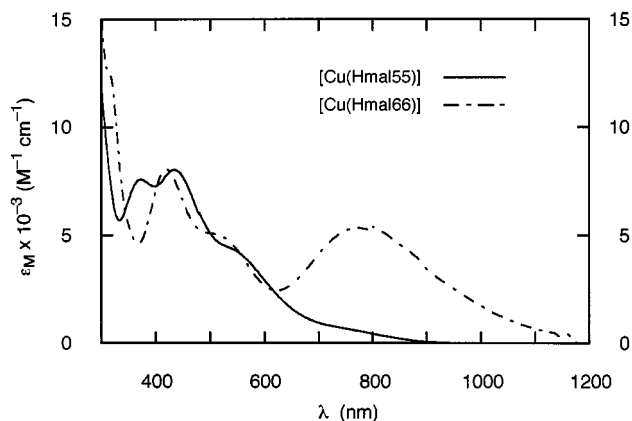


Figure 7. Electronic absorption spectra of a solution of [Cu(Hmal55)] (**3**) and an electrochemically generated solution of [Cu(Hmal66)] in acetonitrile

Complexes **4–12**^[8a,19b,23–26] have the same square-planar CuN₄ coordination environment as complexes **1** and **2**. In addition, complexes **1–10** all contain a malondiamide bridge in the ligand.^[19b,23,24] The type of nitrogen donor group of the two other coordination sites causes the potential to vary by approximately 0.7 V. Thus, a relatively high redox potential (1.34 V) is achieved with π -acceptor ligand donor functions such as pyridine units (**4**),^[23] while the introduction of further negatively charged donor groups in addition to the two already provided by the malondiamide unit affords low potentials (e.g. complex **10**).^[19b] In accordance to this general trend, the redox potentials of **1** and **2** lie between those complexes containing amine donor groups^[19b,23,24] in addition to the malondiamide moiety and that of complex **10**.

The effect of the ring size of the macrocycle on the redox potential is illustrated by the complexes **6**, **8**, and **9**, which contain fifteen-, fourteen-, and thirteen-membered rings, respectively.^[19b,24] Thus, the copper(III) ion is best accommodated by a small ring size, as demonstrated by the low redox potential. A similar trend is also observed in complexes with acyclic ligands where the lowest redox potentials are found with 5-5-5 fused ring systems.^[23] In general agreement with this tendency, the redox potential of **2**, containing a sixteen-membered pseudo-macrocylic ring, is 20 to 45 mV (depending on the employed solvent) higher than that of **1**, in which the pseudo-macrocylic ring is fourteen-membered. Thus, the difference in the redox potential of 45 mV observed in acetonitrile corresponds to a 4.3 kJ mol⁻¹ stabilization of the trivalent oxidation state relative to the divalent oxidation state upon changing the ring size of the pseudo-macrocycle from sixteen in **2** to fourteen in **1**. The long-term instability of the oxidation product of **2** is very likely also related to the facts that the cavity in the sixteen-membered macrocylic ring is too large to accommodate the rather small copper(III) ion and that the already substantially ruffled ligand in copper(II) complex **2** cannot sustain any further ruffling in order to reduce the cavity size after the oxidation of the metal ion.

With respect to the dioximate complex **12**,^[8b] the redox potential of complex **1**, which possesses the same pseudo-

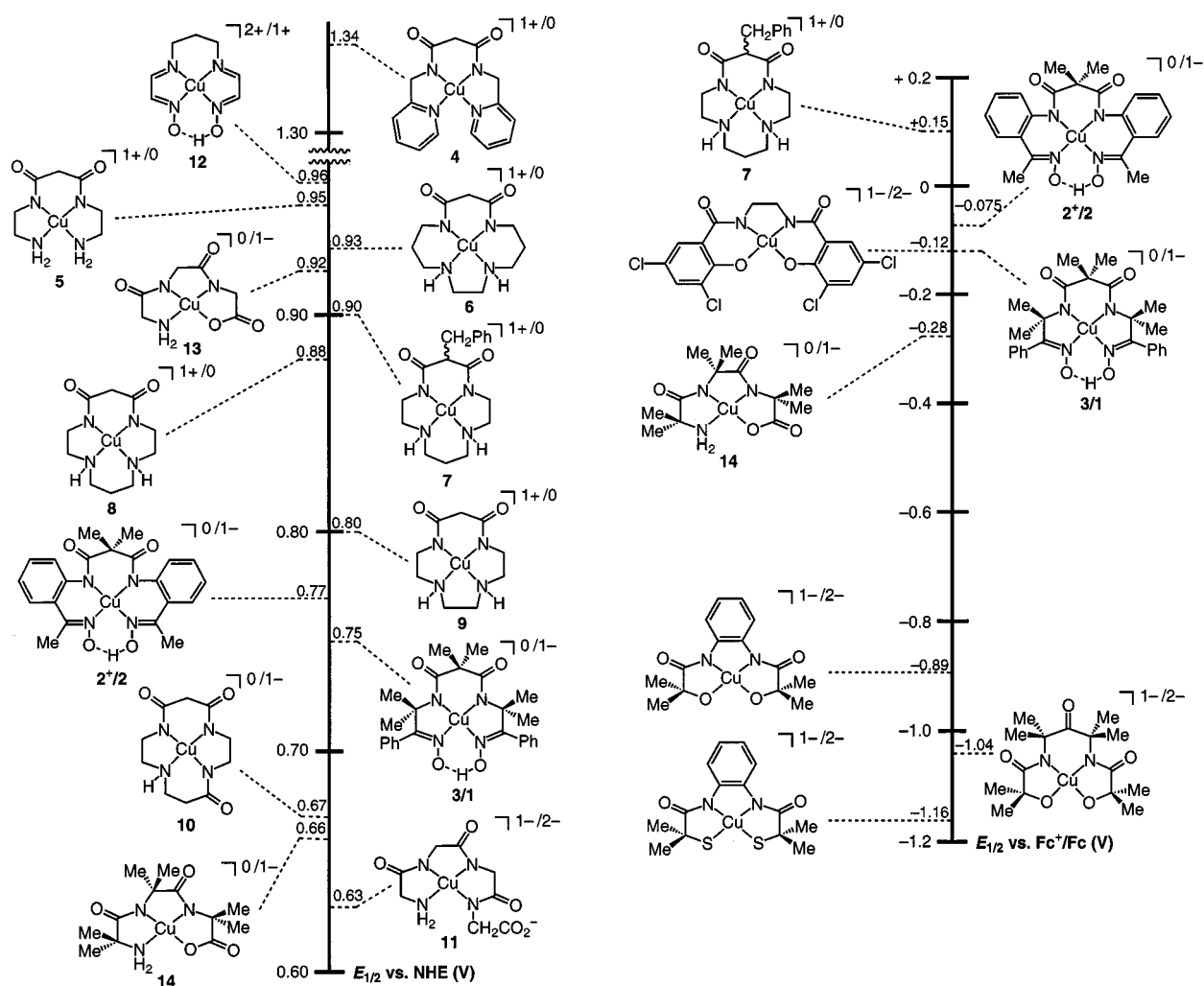


Figure 8. Schematic presentation of the redox potentials of **1** and **2** compared to those of related Cu^{III}/Cu^{II} redox couples in a) water (left) and b) acetonitrile (right). Data are taken from this work and other investigations^[3,4,8a,19b,23–26]

macrocyclic ring size, is lowered by more than 200 mV. This substantial decrease is a testimony of the considerable stabilizing influence that two deprotonated amide functions exert on the high oxidation state of copper ions.

The redox properties of copper(II) peptide complexes were extensively surveyed by Margerum and coworkers.^{[25][26]} The copper(II) complex of the triply deprotonated triglycine ligand (**13**) with a CuN₃O coordination environment is oxidized at 0.92 V.^[25] Substitution of all hydrogen atoms by methyl groups (cf. **14**) causes a substantial decrease of the Cu^{III}/Cu^{II} redox potential.^[26] The presence of methyl groups in α -position to ligand donor atoms may therefore be regarded as another contributing factor to the stabilization of the oxidized complex **3**.

In Figure 8b, the influence on the Cu^{III}/Cu^{II} redox potential of various donor types in combinations with two deprotonated amide donor functions is examined for square planar copper complexes dissolved in acetonitrile. Granting that chelate ring sizes are not always comparable for these complexes, a general trend, however, can still be discerned. Thus, the stabilizing influence of donor groups on the trivalent oxidation state increases in the order amine^[24] < ox-

imate \approx phenolate^[4] < deprotonated amide^[26] < alcoholate^[4] < alkylthiolate.^[3]

Conclusion

Two novel ligands containing two amide and two oxime donor groups were synthesized and their coordination properties were investigated with copper ions. The structure analyses reveal a square-planar coordination geometry around the copper(II) ion in the solid state; this geometry is preserved upon dissolving the complexes in acetonitrile, as indicated by spectroscopic and electrochemical methods. While both amide nitrogen atoms are deprotonated, only one oxime donor group is deprotonated upon coordination of the ligand. The residual oxime hydrogen atom bridges the two *vicinal* oxime oxygen atoms, thereby furnishing the ligand with a pseudo-macrocyclic appearance.

Special emphasis was given to the investigation of the redox properties of the complexes. Thus, both copper(II) compounds can be oxidized to their corresponding copper(III) oxidation states. However, only the oxidation prod-

uct of complex **1** displays sufficient stability to be isolated, resulting in the first structural characterization of a copper(III) complex containing oximes donor functions in its ligand sphere. The coordination geometry around the copper(III) ion is essentially the same as in the reduced complex.

Experimental Section

Methods: $^1\text{H-NMR}$: Varian Gemini 200 and Bruker AM 360, TMS as internal standard. – UV-vis: Varian Cary 5 E. – IR: Perkin-Elmer 1720 FT-IR. – ESR: Bruker ESP 300E. The ESR spectra were analyzed with the programs ESR V1.0 of Frank Neese (Diploma, University of Konstanz, June 1993) and SimFonia 1.2 of Bruker. – Electrochemistry: PAR Model 270 Research Electrochemistry Software controlled Potentiostat/Galvanostat Model 273A with the electrochemical cell placed in a glovebox. Electrochemical experiments were performed on 1–2 mM acetonitrile solutions containing 0.2 M $(\text{Bu}_4\text{N})\text{ClO}_4$ as supporting electrolyte unless otherwise mentioned; a higher than normal electrolyte concentration was applied to minimize solution resistance. All potentials were measured vs. a SCE reference electrode at 25°C. The potentials were not corrected for junction potentials. A Pt-foil electrode was employed as the working electrode. Under these conditions the potential for the ferrocene/ferrocenium ion couple was 0.43 V. Coulometric experiments were performed using a Pt-gauze electrode. – Magnetic susceptibilities: Johnson Matthey Magnetic Susceptibility Balance at room temperature. The values for the diamagnetic susceptibilities of the ligands and the other components of the complexes were taken from the literature.^[27] – Chemical analyses: Chemical analyses were carried out by the analytical laboratory of the authors' institute and by H. Kolbe, Mülheim.

Preparation of Ligands and Complexes. – Materials: 2-Aminoacetophenone (Aldrich), dimethylmalonic acid (Merck), copper(II)-acetate monohydrate (Riedel), and tetraethylammonium acetate tetrahydrate (Fluka) were purchased from the indicated sources and used without further purification. Dimethylmalonyl dichloride^[28] and 2-amino-2-methylpropionophenone hydrochloride^[29] were prepared according to previously published procedures.

***N,N'*-Bis[2-(1-hydroxyimino-2-methyl-1-phenyl)propyl]dimethylmalondiamide Hemihydrate ($\text{H}_4\text{mal55} \times 0.5 \text{ H}_2\text{O}$).** – (a) ***N,N'*-Bis[2-(2-methyl-1-oxo-1-phenyl)propyl]dimethylmalondiamide Monohydrate:** At room temperature, dimethylmalonyl dichloride (2.5 g, 15 mmol) was added dropwise to a stirred solution containing 2-amino-2-methylpropionophenone hydrochloride (7.2 g, 36 mmol) and triethylamine (10.4 mL, 75 mmol) in dichloromethane (150 mL). Stirring of the reaction mixture was continued for 12 h. After the addition of water (30 mL), dichloromethane was added until a clear solution was produced. The organic phase was separated and subsequently washed with 2 N HCl (200 mL), saturated sodium carbonate solution, and water before it was dried over MgSO_4 . Removal of the solvent in vacuo yielded the product as a white solid (4.8 g, 73% yield) which was further recrystallized in EtOH in order to obtain an analytically pure sample. – $\text{C}_{25}\text{H}_{32}\text{N}_2\text{O}_5$ (440.54): calcd. C 68.16, H 7.32, N 6.36; found C 68.21, H 7.38, N 6.58. – $^1\text{H NMR}$ (200 MHz, $[\text{D}_6]\text{Me}_2\text{SO}$): δ = 0.92 (s, CH_3 , 6 H), 1.43 (s, CH_3 , 12 H), 7.32–7.56 (m, Ph–H, 6 H), 7.89 (d, Ph–H, 4 H), 8.00 (s, N–H, 2 H). – IR (KBr): $\tilde{\nu}$ = 3344, 1684, 1644, 1514, 1466, 1447, 1385, 1258, 1217, 1174, 1160, and 718 cm^{-1} (strong bands only). –

(b) ***N,N'*-Bis[2-(1-hydroxyimino-2-methyl-1-phenyl)propyl]dimethylmalondiamide Hemihydrate:** A suspension consisting of *N,N'*-

Bis[2-(2-methyl-1-oxo-1-phenyl)propyl]dimethylmalondiamide monohydrate (2.2 g, 5.0 mmol) and hydroxylammonium chloride (14 g, 201 mmol) in pyridine (150 mL) was stirred for 12 h at 60°C. After removal of the solvent in vacuo, the resulting solid was redissolved in chloroform (200 mL). The chloroform solution was first washed with water (200 mL), then three times with 2 N HCl (100 mL) and finally with water (100 mL). After drying the solution over MgSO_4 , the solvent was evaporated in vacuo to yield the product (1.7 g, 74% yield) as a white solid. – $\text{C}_{25}\text{H}_{33}\text{N}_4\text{O}_{4.5}$ (461.56): calcd. C 65.06, H 7.21, N 12.14; found C 65.02, H 7.00, N 11.83. – $^1\text{H NMR}$ (200 MHz, $[\text{D}_6]\text{Me}_2\text{SO}$): δ = 1.03 (s, CH_3 , 6 H), 1.42 (s, CH_3 , 12 H), 7.02–7.07 (m, Ph–H, 4 H), 7.25–7.37 (m, Ph–H, 6 H), 7.95 (s, 2 H), 10.57 (s, 2 H). – IR (KBr): $\tilde{\nu}$ = 3456, 3312, 2983, 2933, 1663, 1644, 1539, 1512, 1455, 1444, 1420, 1387, 1358, 1216, 1014, 959, 771, 723, and 705 cm^{-1} (strong bands only).

***N,N'*-Bis[2-(1-hydroxyiminoethyl)phenyl]dimethylmalondiamide Monohydrate ($\text{H}_4\text{mal66} \cdot \text{H}_2\text{O}$).** – (a) ***N,N'*-Bis[2-(1-oxoethyl)phenyl]dimethylmalondiamide:** Dimethylmalonyl dichloride (2.02 g, 12 mmol) was slowly dropped into a solution of 2-aminoacetophenone (6.48 g, 48 mmol) in absolute toluene (50 mL) at 0°C. The reaction mixture was warmed to room temperature and stirred for 3 h. The resulting solid was collected by filtration and washed twice with toluene (30 mL). Afterwards, the solid was resuspended under intense stirring for 20 min in an aqueous solution (400 mL) saturated with sodium hydrogen carbonate. After filtration, the solid was washed with copious amounts of water and dried in vacuo at room temperature. Recrystallization of the raw product (3.02 g, 69% yield) from glacial acetic acid yields analytically pure product as a white solid. – $\text{C}_{21}\text{H}_{22}\text{N}_2\text{O}_4$ (366.42): calcd. C 68.84, H 6.05, N 7.65; found C 68.54, H 6.25, N 7.62. – $^1\text{H NMR}$ (200 MHz, $[\text{D}_6]\text{Me}_2\text{SO}$): δ = 1.62 (s, CH_3 , 6 H), 2.65 (s, CH_3 , 6 H), 7.23 (ddd, Ph–H_c, 2 H, J_{ac} = 1.0 Hz, J_{bc} = 7.2 Hz, J_{cd} = 8.1 Hz), 7.63 (ddd, Ph–H_b, 2 H, J_{ab} = 8.6 Hz, J_{bc} = 7.2 Hz, J_{bd} = 1.4 Hz), 8.08 (dd, Ph–H_d, 2 H, J_{bd} = 1.4 Hz, J_{cd} = 8.1 Hz), 8.55 (dd, Ph–H_a, 2 H, J_{ab} = 8.6 Hz, J_{ac} = 1.0 Hz), 11.92 (s, N–H, 2 H). – IR (KBr): $\tilde{\nu}$ = 3215, 1668, 1655, 1607, 1584, 1517, 1479, 1452, 1441, 1384, 1364, 1355, 1314, 1298, 1251, 1226, 1167, 1150, 1122, 961, 910, 762, and 605 cm^{-1} (strong bands only).

(b) ***N,N'*-Bis[2-(1-hydroxyiminoethyl)phenyl]dimethylmalondiamide Monohydrate:** Using a similar procedure as in the synthesis of *N,N'*-Bis[2-(1-hydroxyimino-2-methyl-1-phenyl)propyl]dimethylmalondiamide hemihydrate, *N,N'*-Bis[2-(1-hydroxyiminoethyl)phenyl]dimethylmalondiamide monohydrate was prepared in a 90% yield (3.11 g) in the form of a white solid from *N,N'*-bis[2-(1-oxoethyl)phenyl]dimethylmalondiamide (3.02 g, 8.3 mmol) and hydroxylammonium chloride (21 g, 302 mmol) in pyridine (180 mL). An analytically pure sample was obtained by recrystallization from ethanol. – $\text{C}_{21}\text{H}_{26}\text{N}_4\text{O}_5$ (414.46): calcd. C 60.86, H 6.32, N 13.52; found C 60.53, H 6.53, N 13.67. – $^1\text{H NMR}$ (200 MHz, $[\text{D}_6]\text{Me}_2\text{SO}$): δ = 1.55 (s, CH_3 , 6 H), 2.20 (s, CH_3 , 6 H), 7.16 (ddd, Ph–H_c, 2 H, J_{ac} = 1.1 Hz, J_{bc} = 7.6 Hz, J_{cd} = 7.7 Hz), 7.34 (ddd, Ph–H_b, 2 H, J_{ab} = 8.1 Hz, J_{bc} = 7.6 Hz, J_{bd} = 1.4 Hz), 7.54 (dd, Ph–H_d, 2 H, J_{bd} = 1.4 Hz, J_{cd} = 7.7 Hz), 8.27 (dd, Ph–H_a, 2 H, J_{ab} = 8.1 Hz, J_{ac} = 1.1 Hz), 11.01 (s, 2 H), 11.52 (s, 2 H). – IR (KBr): $\tilde{\nu}$ = 3368, 2925, 1664, 1624, 1580, 1526, 1447, 1394, 1369, 1310, 1295, 1270, 1246, 1124, 1009, 922, and 756 cm^{-1} (strong bands only).

(NEt_4)[Cu(*Hmal55*)] (1**):** A solution was prepared from *Hmal55* \times 0.5 H_2O (231 mg, 0.5 mmol), tetraethylammonium acetate tetrahydrate (261 mg, 1.0 mmol), and copper(II) acetate monohydrate (100 mg, 0.5 mmol) in absolute ethanol (50 mL). After the reaction mixture was heated at reflux for a short time, the solvent was com-

Table 3. Summary of Crystal Data, Intensity Collection and Refinement Parameters for (NEt₄)[Cu(Hmal55)]·0.5 Et₂O (**1**), (NEt₄)[Cu(Hmal66)] (**2**), and [Cu(Hmal55)] (**3**)

Data	1	2	3
formula	C ₃₅ H ₅₄ CuN ₅ O _{4.5}	C ₂₉ H ₄₁ CuN ₅ O ₄	C ₂₅ H ₂₉ CuN ₄ O ₄
<i>M_r</i> [g mol ^{−1}]	680.37	587.21	513.06
crystal dimensions [mm]	0.5 × 0.3 × 0.2	0.6 × 0.5 × 0.5	0.7 × 0.7 × 0.03
crystal system	triclinic	monoclinic	orthorhombic
space group	<i>P</i> 1̄ (No.2)	<i>P</i> 2 ₁ /c (No.14)	<i>Pnma</i> (No.62)
<i>Z</i>	4	4	4
<i>a</i> [Å]	13.317(4)	10.893(3)	9.886(2)
<i>b</i> [Å]	16.311(6)	9.745(2)	25.613(8)
<i>c</i> [Å]	19.162(7)	28.194(8)	9.081(3)
α [deg]	100.42(3)	90	90
β [deg]	102.78(3)	96.86(2)	90
γ [deg]	112.79(2)	90	90
<i>V</i> [Å ³]	3574(2)	2971(1)	2299(1)
ρ_{calc} [g cm ^{−3}]	1.264	1.313	1.482
diffractometer	Hilger & Watts	Syntex P2 ₁	Enraf-Nonius-CAD4
temperature [K]	153	293	153
λ [Å]	0.71073(Mo- <i>K</i> _α)	0.71073(Mo- <i>K</i> _α)	1.54178(Cu- <i>K</i> _α)
μ [cm ^{−1}]	6.56	7.76	16.78
<i>F</i> (000)	1456	1244	1072
scan method	ω -2 θ	ω -2 θ	ω -2 θ
2 θ limits	2.3° ≤ 2 θ ≤ 50.1°	5.1° ≤ 2 θ ≤ 55.1°	6.9° ≤ 2 θ ≤ 152.8°
unique reflections	12444	6851	2481
reflections with <i>F_o</i> > 4 σ (<i>F_o</i>)	8259	4518	2134
number of variables (restraints)	810(5)	438(0)	166(0)
GooF on <i>F</i> ² [a]	1.089	1.120	1.100
<i>R</i> (<i>wR</i> ²), % [a,b,c]	7.05 (17.21)	4.92 (12.56)	5.32 (14.63)

[a] For all reflections with *F_o* > 4 σ (*F_o*). – [b] $R = \sum ||F_o| - |F_c|| / \sum |F_o|$. – [c] $wR^2 = \{\sum [w(F_o^2 - F_c^2)^2] / \sum [w(F_o^2)^2]\}^{1/2}$.

pletely removed in vacuo. The residue was treated with acetonitrile (40 mL) and the resulting red solution was filtered. Slow diffusion of ether into the acetonitrile solution afforded analytically pure product in the form of orange-red needles, which, upon standing, easily lost the ether molecules incorporated in the crystal lattice (234 mg, 73% yield). – C₃₃H₄₉CuN₅O₄ (643.33): calcd. C 61.61, H 7.68, N 10.89; found C 61.31, H 7.68, N 10.81. – Absorption spectrum (acetonitrile): λ_{max} (ϵ_M) 509 (84.4), 405 (141), 260 (sh, 14100), 225 (sh, 25700), and 203 (42500) nm. – IR (KBr): $\tilde{\nu}$ = 2968, 1589, 1493, 1451, 1393, 1362, 1341, 1320, 1199, 1173, 1151, 1089, 1036, 1018, 1010, 923, 886, 825, 785, 737, 699, 656, and 537 cm^{−1} (strong bands only).

(NEt₄)[Cu(Hmal66)] (2**):** In a procedure similar to that described for the synthesis of complex **1**, complex **2** was prepared from H₄mal66 × H₂O (207 mg, 0.5 mmol), tetraethylammonium acetate tetrahydrate (261 mg, 1.0 mmol), and copper(II) acetate monohydrate (100 mg, 0.5 mmol) as dark red blocks (202 mg, 69% yield). – C₂₉H₄₁CuN₅O₄ (587.22): calcd. C 59.32, H 7.04, N 11.93; found C 59.30, H 7.06, N 11.93. – Absorption spectrum (acetonitrile): λ_{max} (ϵ_M) 547 (307), 430 (sh, 501), 310 (sh, 9790), 272 (35500), 251 (sh, 30000), and 223 (24200) nm. – IR (KBr): $\tilde{\nu}$ = 2985, 2950, 1617, 1597, 1586, 1573, 1481, 1439, 1394, 1350, 1304, 1262, 1245, 1174, 1083, 1000, 957, 942, 867, 841, 772, 765, 744, and 530 cm^{−1} (strong bands only).

[Cu(Hmal55)] (3**):** A solution of (NEt₄)[Cu(Hmal55)] (163 mg, 0.25 mmol) in acetonitrile (20 mL) containing 0.1 M NaClO₄ as supporting electrolyte was oxidized at +0.08 V vs Fc/Fc⁺ in an electrochemical cell placed in a glove box. The electrolysis was carried out at a platinum net electrode with a PAR Model 273A Potentiostat/Galvanostat controlled by the PAR Model 270 Research Electrochemistry Software. After the oxidation was completed, the solvent was completely removed in vacuo. The solid was treated with toluene (30 mL) and the resulting dark red-brown solution was filtered. Hexane (120 mL) was layered upon the solution. Slow mixing of

the two layers by diffusion afforded analytically pure product in the form of dark red blocks (64.5 mg, 51% yield). – C₂₅H₂₉CuN₄O₄ (513.08): calcd. C 58.52, H 5.70, N 10.92; found C 58.38, H 5.76, N 10.88. – ¹H NMR (360 MHz, CD₂Cl₂): δ = 1.36 (s, CH₃, 6 H), 1.64 (s, CH₃, 12 H), 7.27 (m, Ph–H, 6 H), 7.48 (m, Ph–H, 4 H), 16.68 (s, N=OH, 1 H). – Absorption spectrum (acetonitrile): λ_{max} (ϵ_M) 700 (sh, 944), 533 (sh, 4460), 436 (8030), 373 (7590), 279 (17700), and 242 (15900) nm. – IR (KBr): $\tilde{\nu}$ = 2986, 2937, 1617, 1593, 1560, 1452, 1394, 1371, 1362, 1351, 1224, 1200, 1124, 879, 747, and 700 cm^{−1} (strong bands only).

Solutions of [Cu(Hmal66)]: For the purpose of comparing spectroscopic data, solutions of the oxidation product of **2** in acetonitrile were electrochemically generated in situ at an applied potential of 0.125 V vs Fc/Fc⁺ and, in light of the apparent instability of the oxidized species, immediately used for the respective measurements. Absorption spectrum (acetonitrile): λ_{max} (ϵ_M) 773 (5350), 500 (sh, 5100), 420 (8040), 313 (sh, 12600), 269 (35200), and 243 (35400) nm.

Crystal Structure Analyses of the Copper Complexes: Table 3 contains the cell parameters of the crystals and experimental details on the data collections and structure refinements. The positions of the non-hydrogen atoms were determined by SHELXS 86^[30] and by Fourier difference maps using the program SHELXL-93 (**1** and **2**) or SHELXL-97 (**3**).^[30] The structural parameters were refined with the program SHELXL-93 or SHELXL-97, using *F*² of all symmetry-independent reflections except those with very negative *F*²-values. Empirical absorption correction on the data set of **3** was applied by using the program DIFABS. All non-hydrogen atoms were refined anisotropically unless stated otherwise. The ether molecule in **1**·0.5 Et₂O is disordered and the atoms of this crystal solvent are therefore ill defined, resulting in large temperature factors and somewhat distorted bond lengths. The non-hydrogen atoms of this molecule were therefore refined isotropically. The tetraethylammonium cation in **2** is disordered and was modeled by two separate

molecules. Half of the complex **3** is related to the other half by a symmetry plane passing through the copper atom and the atoms of the dimethylmethylene group of the dimethylmalondiamide unit. Hydrogen atoms were assigned idealized locations and their isotropic temperature factors were refined, except for those bound to the oxime oxygen atoms in **1**, in which complex the positions and the isotropic temperature factors were refined. The locations of the hydrogen atoms which asymmetrically bridge both oxime oxygen atoms in **2** and **3** are disordered over two positions.

The largest peaks (holes) in the final difference Fourier maps correspond to 1.13 (−1.12) e Å^{−3}, 0.56 (−0.45) e Å^{−3}, and 0.68 (−0.67) e Å^{−3} for structures analyses of **1**, **2**, and **3**, respectively.

Crystallographic data (excluding structure factors) for the structures reported in this paper have been deposited with the Cambridge Crystallographic Data Center as supplementary publication no. CCDC-101423. Copies of the data can be obtained free of charge on application to The Director, CCDC, 12 Union Road, Cambridge CB2 1EZ, UK (Fax: Int. code +44 (1223) 336-033; E-mail: deposit@chemcrs.cam.ac.uk).

Acknowledgments

We thank the Deutsche Forschungsgemeinschaft for financial support.

- [1] [1a] D. W. Margerum, *Pure Appl. Chem.* **1983**, *55*, 23–34. — [1b] D. W. Margerum, G. D. Owens, *Met. Ions Biol. Syst.* **1981**, *12*, 75–132.
- [2] L. L. Diaddario, W. R. Robinson, D. W. Margerum, *Inorg. Chem.* **1983**, *22*, 1021–1025.
- [3] J. Hanss, H.-J. Krüger, *Angew. Chem.* **1996**, *108*, 2989–2991; *Angew. Chem. Int. Ed. Engl.* **1996**, *35*, 2827–2830.
- [4] F. C. Anson, T. J. Collins, T. G. Richmond, B. D. Santarsiero, J. E. Toth, B. G. R. T. Treco, *J. Am. Chem. Soc.* **1987**, *109*, 2974–2979.
- [5] P. J. M. W. L. Birker, *Inorg. Chem.* **1977**, *16*, 2478–2482.
- [6] A. Chakravorty, *Coord. Chem. Rev.* **1974**, *13*, 1–46.
- [7] [7a] R. S. Drago, E. I. Baucom, *Inorg. Chem.* **1972**, *11*, 2064–2069. — [7b] A. Chakravorty, *Isr. J. Chem.* **1985**, *25*, 99–105. — [7c] G. Sproul, G. D. Stucky, *Inorg. Chem.* **1973**, *12*, 2898–2902. — [7d] J.-M. Bemtgen, H.-R. Gimpert, A. von Zelewski, *Inorg. Chem.* **1983**, *22*, 3576–3580.
- [8] [8a] Y. Sulfab, N. I. Al-Shatti, *Inorg. Chim. Acta* **1984**, *87*, L23–L24. — [8b] Y. Sulfab, M. A. Hussein, N. I. Al-Shatti, *Inorg. Chim. Acta* **1982**, *67*, L33–L34.
- [9] [9a] D. Luneau, H. Oshio, H. Okawa, S. Kida, *Chem. Lett.* **1989**, 443–444. — [9b] H. Okawa, M. Koikawa, S. Kida, D. Luneau, H. Oshio, *J. Chem. Soc., Dalton Trans.* **1990**, 469–475. — [9c] D. Luneau, H. Oshio, H. Okawa, S. Kida, *J. Chem. Soc., Dalton Trans.* **1990**, 2283–2286. — [9d] D. Luneau, H. Oshio, H. Okawa, M. Koikawa, S. Kida, *Bull. Chem. Soc. Jpn.* **1990**, *63*, 2212–2217. — [9e] P. Chaudhuri, M. Winter, B. P. C. Della Védova, E. Bill, A. Trautwein, S. Gehring, P. Fleischhauer, B. Nuber, J. Weiss, *Inorg. Chem.* **1991**, *30*, 2148–2157. — [9f] R. Ruiz, J. Sanz, B. Cervera, F. Lloret, M. Julve, C. Bois, J. Faus, M. C. Muñoz, *J. Chem. Soc., Dalton Trans.* **1993**, 1623–1628. — [9g] F. Birkelbach, M. Winter, U. Flörke, H.-J. Haupt, C. Butzlaff, M. Lengen, E. Bill, A. X. Trautwein, K. Wieghardt, P. Chaudhuri, *Inorg. Chem.* **1994**, *33*, 3990–4001. — [9h] R. Ruiz, F. Lloret, M. Julve, M. C. Muñoz, C. Bois, *Inorg. Chim. Acta* **1994**, *219*, 179–186. — [9i] P. Chaudhuri, M. Winter, U. Flörke, H.-J. Haupt, *Inorg. Chim. Acta* **1995**, *232*, 125–130.
- [10] O. Kahn, *Struct. Bonding (Berlin)* **1987**, *68*, 89–167.
- [11] H.-J. Krüger, G. Peng, R. H. Holm, *Inorg. Chem.* **1991**, *30*, 734–742.
- [12] [12a] A. M. Duda, A. Karaczyn, H. Kozłowski, I. O. Fritsky, T. Glowiak, E. V. Prisyazhnaya, T. Y. Sliva, J. Swiatek-Kozłowska, *J. Chem. Soc., Dalton Trans.* **1997**, 3853–3859. — [12b] C. O. Onindo, T. Y. Sliva, T. Kowalik-Jankowska, I. O. Fritsky, P. Buglyo, L. D. Pettit, H. Kozłowski, T. Kiss, *J. Chem. Soc., Dalton Trans.* **1995**, 3911–3915.
- [13] J. Hanss, H.-J. Krüger, *Angew. Chem.* **1998**, *110*, 366–369; *Angew. Chem. Int. Ed. Engl.* **1998**, *37*, 360–363.
- [14] T. J. Collins, *Acc. Chem. Res.* **1994**, *27*, 279–285.
- [15] [15a] H. C. Freeman, M. R. Taylor, *Acta Crystallogr., Sect. B* **1965**, *18*, 939–952. — [15b] T. Toki, M. Mikuriya, H. Okawa, I. Murase, S. Kida, *Bull. Chem. Soc. Jpn.* **1984**, *57*, 2098–2105.
- [16] [16a] J. A. Bertrand, J. H. Smith, D. G. VanDerveer, *Inorg. Chem.* **1977**, *16*, 1484–1488. — [16b] E. Frasson, R. Bardi, S. Bezzi, *Acta Crystallogr.* **1959**, *12*, 201–205. — [16c] O. P. Anderson, C. M. Perkins, K. K. Brito, *Inorg. Chem.* **1983**, *22*, 1267–1273.
- [17] J. Peisach, W. E. Blumberg, *Arch. Biochem. Biophys.* **1974**, *165*, 691–708.
- [18] A. B. P. Lever, *Inorganic Electronic Spectroscopy*, 2nd ed., Elsevier, Amsterdam, **1984**, 554–572.
- [19] Using a nonisothermal cell, the Cu^{III}/Cu^{II} redox potential shifts by maximally +10 mV upon changing the temperature from −30 to +30°C. If preferential axial coordination of solvent molecules to the copper(II) ion occurs, shifts of −30 to −50 mV are expected: [19a] M. P. Youngblood, D. W. Margerum, *Inorg. Chem.* **1980**, *19*, 3068–3072. — [19b] E. Kimura, T. Koike, R. Machida, R. Nagai, M. Kodama, *Inorg. Chem.* **1984**, *23*, 4181–4188.
- [20] E. L. Solomon, K. W. Penfield, D. E. Wilcox, *Struct. Bond. (Berlin)* **1983**, *53*, 1–57.
- [21] The absorption bands in the spectra of the copper(III) complexes vanish over time without new characteristic absorption bands appearing. The resulting spectra do not resemble those of the respective original copper(II) complexes indicating, that decomposition of the complexes has occurred.
- [22] A. W. Hamburg, D. W. Margerum, *Inorg. Chem.* **1983**, *22*, 3884–3893.
- [23] T. Sakurai, J.-I. Hongo, A. Nakahara, Y. Nakao, *Inorg. Chim. Acta* **1980**, *46*, 205–210.
- [24] L. Fabbrizzi, A. Perotti, A. Poggi, *Inorg. Chem.* **1983**, *22*, 1411–1412.
- [25] F. P. Bossu, K. L. Chellappa, D. W. Margerum, *J. Am. Chem. Soc.* **1977**, *99*, 2195–2203.
- [26] S. T. Kirksey, Jr., T. A. Neubecker, D. W. Margerum, *J. Am. Chem. Soc.* **1979**, *101*, 1631–1633.
- [27] [27a] *Landolt-Börnstein Vol II/10* (6th edition) (Eds.: K.-H. Hellwege, A. M. Hellwege), Springer Verlag, Berlin, **1967**. — [27b] *Landolt-Börnstein New Series Vol II/8 Supplement 1* (Eds.: K.-H. Hellwege, A. M. Hellwege), Springer Verlag, Berlin, **1976**.
- [28] I. Smedley, *J. Chem. Soc.* **1910**, *97*, 1475–1494.
- [29] S. Gabriel, *Chem. Ber.* **1911**, *44*, 57–69.
- [30] *SHELXS-86*: Crystal Structure Solution Program, G. M. Sheldrick, Göttingen, **1986**. G. M. Sheldrick, in *Crystallographic Computing 3*, G. M. Sheldrick, C. Krüger, R. Goddard, Eds.; Oxford University Press, **1985**; pp. 175. — *SHELXL-93*: Crystal Structure Refinement Program, G. M. Sheldrick, Göttingen, **1993**. — *SHELXL-97*: Crystal Structure Refinement Program, G. M. Sheldrick, Göttingen, **1997**.

Received May 8, 1998
[198144]